Received: 7 June 2022 | Revised: 30 August 2022 | Accepted: 5 September 2022

DOI: 10.1002/jcc.27002

RESEARCH ARTICLE

Journal of COMPUTATIONAL CHEMISTRY WILEY

On the origin of photodynamic activity of hypericin and its iodine-containing derivatives

Bruna Clara De Simone | Gloria Mazzone | Marirosa Toscano | Nino Russo

Department of Chemistry and Chemical Technologies, University of Calabria, Rende, Italy

Correspondence
Nino Russo, Department of Chemistry and Chemical Technologies, University of Calabria, 87036 Rende (CS), Italy.
Email: nrusso@unical.it

Abstract

The main photophysical properties, useful for establishing whether hypericin in anionic form and some of its derivatives containing heavy atoms such as iodine, can be proposed for their use in photodynamic therapy, were determined using density functional based computations. The results showed that in the anionic form and in the iodinated derivatives, the absorption wavelength undergoes a bathochromic shift, the singlet-triplet energy gap assumes values that allow to excite the oxygen molecule from its ground to the excited singlet state, and that the spin–orbit couplings between singlet and triplet states significantly increase.

KEYWORDS
DFT, hypericin, PDT, photophysical properties, spin–orbit coupling constants

1 | INTRODUCTION

Hypericin, a natural molecule extracted from several species of the genus *Hypericum*, is used since ancient times for healing purposes. The first documented records of its medical use date back to around 200 BC and over the centuries it has been used as a drug in various medical applications. Since its isolation in 1911,[1] the phenanthroperylene type structure of hypericin has been the subject of a huge amount of investigation. In fact, the structural knowledge of multiple hydroxyl derivative of phenanthroperylene systems is difficult to determine due the presence of tautomerization, protonation and dissociation and torsional equilibria.[2] However, the great mole of theoretical and experimental studies has finally well established the structural properties of hypericin under different chemical conditions.[3–6]

The interest in this molecule has increased in recent decades due to the discovery of its antiviral, antimicrobial, anti-inflammatory and anticancer effects.[7–9] Furthermore, its photophysical properties make it a powerful and natural photosensitizer that can be used in photodynamic therapy (PDT)[10] for the treatment of psoriasis, disinfection from viruses and bacteria and, more recently, in oncology where his study is in the clinical and pre-clinical phase for the treatment of different types of tumors.[7]

PDT is a well-established clinical treatment based on a photophysical cycle. After the photosensitizer has been positioned in the target, it is excited in its singlet state (transition S_0 to $>S_1$) by irradiation with light of appropriate wavelength. Since the penetration capacity in the tissue is a function of the wavelength of the radiation, excitations with light in the band between 500 and 800 nm (the so-called therapeutic window) are optimal for the treatment of solid tumors. For disinfection applications against microbes or viruses, irradiations with lower wavelengths capable of destroying their thin membranes are also effective. Once irradiated, if the PS used is fluorescent, it returns to the ground state (S_0), otherwise it can transfer its energy to an excited triplet state (T_1) through an intersystem crossing (ISC) mechanism that can only occur if the spin–orbit between the two states (S/T) assumes consistent values. At this point, the T_1 state, if its energy is greater than 0.98 eV, in the presence of molecular oxygen, can transfer its energy to the oxygen causing the excitation of O_2 from the ground triplet state to the excited singlet one, a strong cytotoxic agent able to destroy the tissues.

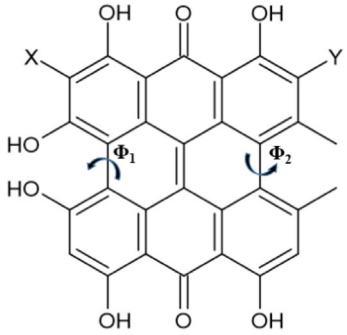

X = H, Y= H **hyp**
X = I, Y = H **hyp-I**
X = H, Y = I **hyp-I2**

SCHEME 1 Schematic representation of the investigated compounds and definition of torsional angles

Recently it has been proposed that the PDT action of hypericin depends on its anionic form which is dominantly present in aqueous solution and possesses photophysical properties different from its neutral form.[11] Stimulated by this hypothesis, we have undertaken a theoretical study of the photophysical properties of both forms by calculating the geometries of the states involved, the excitation energies, the entity of the SOCs and the energy differences between their ground and triplet states ($\Delta E_{S\text{-}T}$).

Since in the literature it is widely demonstrated that the presence of heavy atoms can increase SOCs[12–15] and then the ISC rate, we carried out the same calculations for the neutral and anionic forms of hypericin containing iodine atom in different positions of its skeleton (Scheme 1).

The study was performed by using the density functional theory (DFT) and its time dependent version (TDDFT).

2 | COMPUTATIONAL DETAILS

For this study, we chosen a theoretical computation protocol, widely used previously to determine the photophysical properties of organic and inorganic systems active in PDT,[16–18] and of which we report the most significant details below.

All the geometries were optimized by using the M06 exchange-correlation functional[19] coupled with the 6-31G(d) basis sets for all the atoms and the SDD pseudopotential[20] for iodine. SMD solvation model[21] was used considering the DMSO solvent (due to the presence in the literature of the electronic spectra provided in this environment). No symmetry constraints were imposed during the geometry optimizations. In order to verify if the obtained structures were real minima, frequencies calculations were performed at the same level of theory. Vertical excitation energies were obtained at the M06/6-31+G(d)//M06/6-31G(d) level of theory. All the data have been obtained through the use of the Gaussian 09 code.[22]

The spin–orbit couplings (SOCs) defined as:

$$\mathrm{SOC}_{nm} = \sqrt{\sum_i \left|\left\langle \psi_{S_n} \middle| \hat{H}_{SO} \middle| \psi_{T_{i,m}} \right\rangle\right|^2};\ i = x, y, z$$

where $\hat{H}_{SO}$ is the spin–orbit Hamiltonian, were computed with the DALTON code[23] by using the spin–orbit coupling operators for effective core potentials with an effective nuclear charge[24] for iodine atoms containing systems. The atomic mean field approximation[25] was used in the other cases. For this purpose, the B3LYP functional[26,27] was employed in conjunction with the cc-pVDZ basis set for all the atoms except for iodine for which we adopted the corresponding pseudopotential.

3 | RESULT AND DISCUSSION

3.1 | Geometries

The optimized ground state geometry structures are depicted in Figure 1 (front and side views), while in Table 1 the ϕ_1 and ϕ_2 dihedral angle values are reported.

From our and previous studies on the structural properties on the neutral hypericin (**hyp**), it is clear that the most stable structure (ground state) is that in which the carbonyl groups are in position C_7 and C_{14}. The structure appears slightly distorted with a consistent helical twist ($\phi_1 = 31.2^\circ$ and $\phi_2 = 32.9^\circ$) as also found in the previous x-ray[28] and theoretical investigation.[3,4] This characteristic is essentially due to the steric hindrance between the OH moieties in the *bay* region and between the two methyl groups in the *peri* site. From the determined p*K*a values[29,30] and from previous theoretical studies,[3–5] it was established that the first deprotonation takes place at the expense of an OH group in the *bay* region. The structure of the obtained anion (**hyp**$^-$) still presents structural distortions ($\phi_1 = 30.3^\circ$ and $\phi_2 = 33.2^\circ$) which are similar to those found in the corresponding neutral though the OH—OH repulsion in the *bay* region is not present in the anionic form. Also for **hyp**$^-$ our optimized structure (Table 1 and Figure 1) well agrees with the previous x-ray[28] and DFT results.[3–5,11] Similar distorted structures (Table 1) have been found for neutral and anionic compounds containing iodine although for **hyp-I2** and **hyp-I2**$^-$ systems, the corresponding ϕ_1 values are smaller.

The excited S_1 and T_1 and T_2 states topologies are similar to the ground one. In particular, the two triplets present small variations (the two torsional angles differences are contained in a range of 6–8 degree) and this also reflect their similar molecular orbital pictures.

3.2 | Excitation energies

The computed lowest excitation energies, of interest for our purposes, are given in Table 2 together with the oscillator strength and the orbitals involved in the transitions.

For neutral hypericin **hyp**, the computed wavelength for the S_1 state (537 nm) is in good agreement with previous theoretical B3LYP computations (556[3] and 560 nm[11]) and experimental value in ethanol solvent.[31] Below such state lie two triplet states at 719 nm (1.73 eV) and 595 nm (2.08 eV). For the first of them, the comparison with the

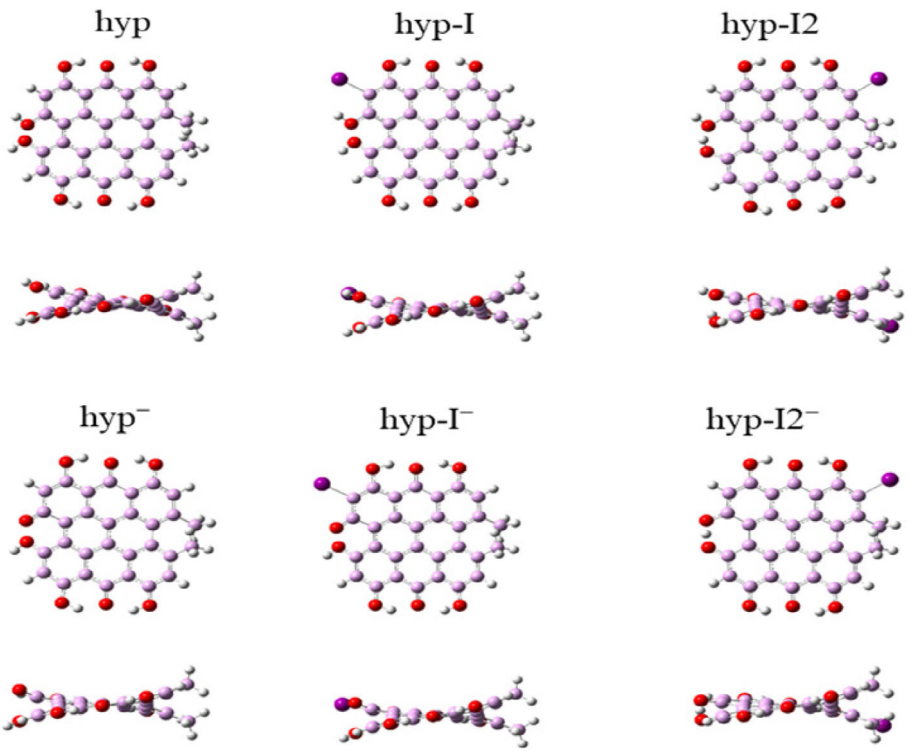

FIGURE 1 Front and side views for the optimized structures of the studied compounds

TABLE 1 Ground (GS) and excited states (*S*, *T*) dihedral angle values for the studied compounds in DMSO solvent

hyp	**GS**	S_1	T_1	T_2	**hyp−**	**GS**	S_1	T_1	T_2
Φ_1	31.2	29.3	28.8	34.1		30.3	29.8	29.2	-
Φ_2	32.9	30.8	30.5	36.4		33.2	32.8	32.4	-
hyp-I					**hyp-I** $^-$				
Φ_1	32.0	30.1	29.6	35.0		30.9	30.0	29.4	-
Φ_2	32.8	30.4	30.1	36.3		33.2	32.2	31.9	-
hyp-I2					**hyp-I2**$^-$				
Φ_1	27.6	25.6	25.2[a]	25.2[a]		19.3	21.9	16.7	22.1
Φ_2	33.9	31.3	30.9	30.9		34.5	32.9	32.7	36.7

[a]Degenerate states.

experimental data obtained from phosphorescence spectra in ethanol (730 nm)[32] and acetonitrile (752 nm)[33] and with the theoretical one calculated at B3LYP level (765 nm)[3] are pretty good. Both these triplets have a ΔES_1-T_n energy gap higher than that necessary to excite O_2 in its $^1\Delta_g$ state.

The deprotonation in the *bay* region, that gives rise to the **hyp**$^-$ anion, causes a bathochromic shift of S_1 up to 588 nm, which is in excellent agreement with the experimental value (590 nm)[34] and with the previous B3LYP theoretical evaluation (581 nm).[11] Also, T_1 undergoes the same phenomenon. Contrary to **hyp**, its anionic form does not possess an additional triplet state useful for PDT. The mono- and di-iodination of the neutral hypericin (**hyp-I** and **hyp-I2**) does not cause significant shift in the values of S_1, T_1, and T_2 which are within 10 nm. The same trend is found in the iodinated compounds of the **hyp**$^-$ anion (**hyp-I**$^-$ and **hyp-I2**$^-$) as it is evident from Table 2.

A general trend that can be deduced from our results is the non-negligible bathochromic shift (about 0.2 eV) that the presence of the negative charge provokes in the T_1 states of all the investigated molecules. From Table 2 it can be seen how, for all the studied systems, the excited states S_1 and T_1 originate from a transition HOMO → LUMO while the T_2 ones derive from an HOMO − 1 → LUMO one.

In order to verify if the used solvation model is able to give reliable results, we have redone the calculations for **hyp**$^-$, by adding one or two explicit solvent molecules (DMSO) to the used solvation model. The results, (see Table S1) show how, for both excited states S_1 and T_1, the differences with respect to the SMD continuum model vary by a few nm (maximum 3 nm for S_1 and 7 nm for T_1). If we consider the bathochromic shift that occurs, for the S_1 state, in going from the neutral to the anionic form of hypericin, we note that it does not undergo significant variations depending on the model used, as the

TABLE 2 Vertical excitation energy, ΔE (eV), λ (nm), oscillator strength f and main transitions for the studied compounds computed in DMSO using M06/6-31+G(d)//M06/6-31G(d)

Molecule	State	λ	ΔE	f	Main transition
hyp	S_1	537	2.31	0.383	H → L, 98%
	T_1	719	1.73		H → L, 98%
	T_2	595	2.08		H-1 → L, 88%
hyp$^-$	S_1	588	2.11	0.256	H → L, 98%
	T_1	825	1.50		H → L, 98%
hyp-I	S_1	539	2.30	0.409	H → L, 98%
	T_1	721	1.72		H → L, 98%
	T_2	604	2.05		H-1 → L, 84%
hyp-I$^-$	S_1	577	2.15	0.256	H → L, 95%
	T_1	815	1.52		H → L, 98%
hyp-I2	S_1	542	2.29	0.410	H → L, 98%
	T_1	718	1.72		H → L, 98%
	T_2	617	2.01		H-1 → L, 85%
hyp-I2$^-$	S_1	544	2.29	0.297	H → L, 98%
	T_1	761	1.63		H → L, 98%
	T_2	575	2.16		H-1 → L, 78%

values obtained are 51, 50, and 48 nm for **hyp**$^-$, **hyp**$^-$ + **H$_2$O**, and **hyp**$^-$ + **2H$_2$O**, respectively.

3.3 | Photodynamic action

In order to exert the photodynamic action, the photosensitizers have to possess a triplet state lying at least 0.98 eV under the ground singlet one and a favorable ISC kinetic for its population. In the limit of Frank–Condon approximation and in the non-adiabatic regime, the K_{ISC} of the S_n-T_m transitions can be estimated by using the Fermi Golden rule assuming that both the involved electronic states are harmonic[35]:

$$k_{ISC}^{nm} = \frac{2\pi}{\hbar}\langle \psi_{S_n} | \hat{H}_{SO} | \psi_{T_m} \rangle^2 \times \text{FCWD}$$

in this expression $\hat{H}_{SO}$ is the spin–orbit Hamiltonian and FCWD is the Franck–Condon weighted density of states that is proportional to the exponential factor[35]:

$$\text{FCWD} \propto \exp\left[-\frac{(\Delta E_{S-T})^2}{4\lambda k_B T}\right]$$

being λ the Marcus reorganization energy and $\Delta E_{S\text{-}T}$ the difference between the energies of singlet and the triplet states.

As previously mentioned, efficient ISC can be obtained if the relative SOCs assumes non-negligible values. As a reference we can consider the Foscan® (5,10,15,20-tetrakis-[m-hydroxyphenyl]chlorin), approved for its use in PDT medical treatments,[36] and whose spin–orbit coupling constant $\langle S_1|H_{SO}|T_1\rangle$ has been computed to be 0.24 cm^{-1}.[37]

The $\langle S_1|H_{SO}|T_1\rangle$ and $\langle S_1|H_{SO}|T_2\rangle$ computed for hypericin systems are reported in Table 3. From this table, we can observe that in **hyp**, which has a very small SOC value (0.03 cm^{-1}), the relative ISC is unlikely to occur. On the contrary, in **hyp**$^-$ where the SOC results to be 0.84 cm^{-1} (higher than that obtained for the Foscan®) the $S_1 \rightarrow T_1$ ISC should take place. As expected, because of heavy atom effect, the SOC values calculated for the neutral, **hyp-I** and **hyp-I2**, and charged iodinated species, are sensibly higher than those of **hyp** and its anion. Therefore, in principle they can better work as photosensitizer in PDT than the heavy atom free hypericin. Furthermore, the SOC values for $S_1 \rightarrow T_2$ radiationless transition are systematically higher than $S_1 \rightarrow T_1$ one and increase significantly in the iodine containing systems. Also in the case of both anionic iodine-containing systems, the S_1/T_1 SOCs are higher than that in the corresponding neutral form. In all cases, the computed SOCs remain considerably higher than those of iodine-free hypericin.

According to the El Sayed rules,[38] SOCs values increase when the symmetry of the molecular orbitals (MO) involved in the transition changes significantly. This means that $\langle S_{(\pi\pi^*)}|\hat{H}_{so}|T_{(\pi\pi^*)}\rangle$ have small SOSs with respect to $\langle S_{(n\pi^*)}|\hat{H}_{so}|T_{(\pi\pi^*)}\rangle$. To verify the existence of this relationship in the studied compounds, we plotted the molecular orbitals involved in the main transitions reported in Table 2. Figure 2 report the MOs for **hyp**, **hyp**$^-$ and **hyp-I**, while those for the remaining systems are reported in Figure S1. From these Figures, it can be seen that the orbital symmetries do not vary too much and that they have a $\pi\pi^*$ nature. This explains why the computed SOC values are smaller than those previously calculated for other systems containing heavy atoms.[12–18] Although this is general, the increase in SOC values can be partially explained. In **hyp**, only in the HOMO − 1 → LUMO orbitals, which characterize the T_2 state, there is a small variation in their composition that can justify the increased value of $\langle S_1|\hat{H}_{so}|T_2\rangle$. In **hyp**$^-$, the increase in SOC for ISC from S_1 to T_1 can be explained in the same way, since a participation of iodine in the MO surfaces can be observed. A similar situation is found for **hyp-I** but the significant increase in SOCs is also due to the iodine presence. In fact, the spin–orbit coupling matrix elements depend also on the effective nuclear charge of heavy atoms with the amplitude of the spin–orbit interaction proportional to $Z_{eff.}$[4]

From the equation reported for K_{ISC} it appears clear that, although the kinetic constant depends considerably on the spin–orbit coupling matrix elements, also the energy difference between the two considered electronic states should be considered to establish the fastest and more efficient deactivation pathways.

For **hyp**$^-$ and **hyp-I**$^-$ in which only the

$$S_0 \xrightarrow{A} S_1 \xrightarrow{ISC} T_1,$$

deactivation channel is possible and due to the fact that the $\Delta E_{S\text{-}T}$ values are very similar (0.61 and 0.63 eV for **hyp**$^-$ and **hyp-I**$^-$, respectively) the fastest ISC is dictated by the SOC value that

TABLE 3 Spin–orbit matrix elements (cm^{-1}) and $\Delta E_{S\text{-}T}$ (eV) calculated at the B3LYP/cc-pVDZ//M06/6-31G(d) level of theory

SOC ($\Delta E_{S\text{-}T}$)	hyp	hyp$^-$	hyp-I	hyp-I$^-$	hyp-I2	hyp-I2$^-$
$\lvert\langle\Psi_{S_1}\lvert\hat{H}_{so}\rvert\Psi_{T_1}\rangle\rvert$	0.03 (0.58)	0.84 (0.61)	5.57 (0.58)	14.0 (0.63)	2.3 (0.57)	12.6 (0.66)
$\lvert\langle\Psi_{S_1}\lvert\hat{H}_{so}\rvert\Psi_{T_2}\rangle\rvert$	0.40 (0.23)		31.96 (0.25)		61.0 (0.13)	8.5 (0.13)

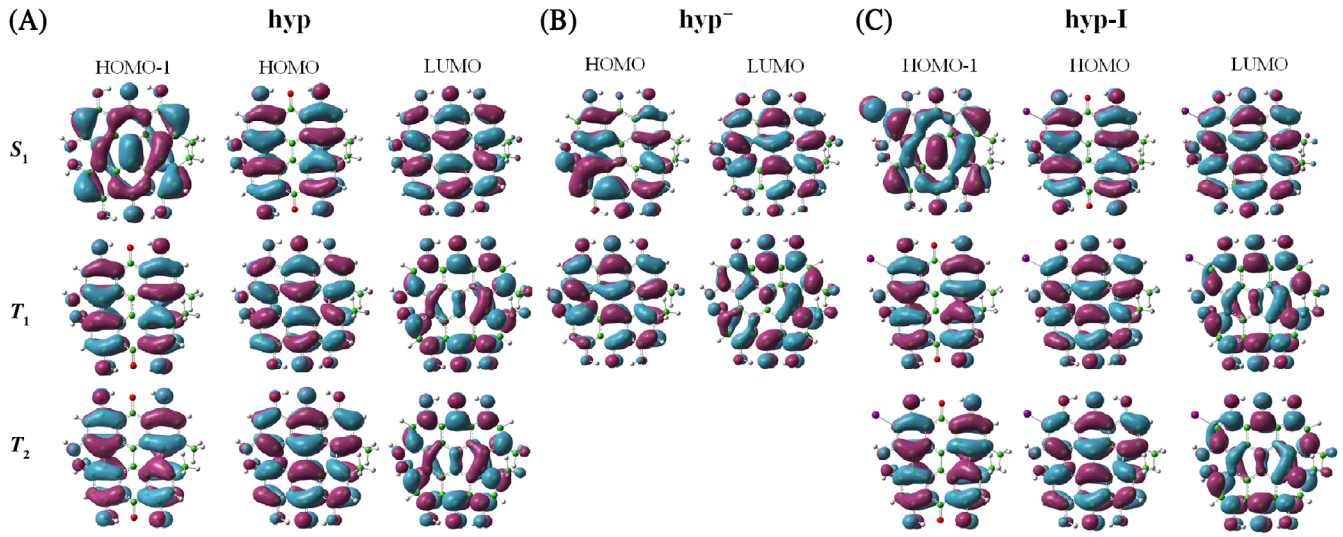

FIGURE 2 Molecular orbitals contour plot (isovalue 2×10^{-2} a.u.) for excited states of (A) **hyp**, (B) **hyp**$^-$, and (C) **hyp-I**

in the case of the iodinated system results to be higher of more one order of magnitude.

For the other studied molecules, the deactivation paths can be essentially two:

$$(\mathrm{i})\, S_0 \xrightarrow{A} S_1 \xrightarrow{ISC} T_1; (\mathrm{ii})\, S_0 \xrightarrow{A} S_1 \xrightarrow{ISC} T_2 \xrightarrow{IC} T_1.$$

Looking on the $\Delta E_{S\text{-}T}$ values reported in Table 2, the second mechanism seems to be more probable because of the higher SOCs, the lower singlet-triplet energy gaps and the fact that the IC process between the two triplet states it is always much faster.

4 | CONCLUSIONS

The photophysical properties of hypericin and iodine-containing derivatives in the form of neutral and anionic species, are here reported aiming at establishing the most active form and the influence of the heavy atom presence on the photodynamic action. On the basis of the theoretical investigation, the following conclusions can be drawn:

1. the computed spin orbit coupling constants of the anionic form of the hypericin are higher than those of the neutral species and, since in aqueous environment anionic form is the most abundant, we can claim that it is responsible for PDT activity;
2. the presence of a heavy halogen atom in the skeleton increases the possible PDT activity for both neutral and deprotonated species;
3. the most probable deactivation pathway is that in which the S_1-T_2 intersystem crossing is followed by a T_2-T_1 interconversion.

We hope that our results can stimulate desirable future studies on the possible applications of these systems in photodynamic therapy.

ACKNOWLEDGMENT

The authors thank the Dipartimento di Chimica e Tecnologie Chimiche, Università della Calabria for the support. Open Access Funding provided by Universita della Calabria within the CRUI-CARE Agreement.

CONFLICT OF INTEREST

The authors declare no conflict of interest.

DATA AVAILABILITY STATEMENT

The Gaussian 09 package[22] was used for structural optimization, frequencies, and excited states calculations. The DALTON code[23] was used for the spin orbit coupling computations. The optimized structures are reported in the Supporting Information section.

ORCID

Nino Russo https://orcid.org/0000-0003-3826-3386

REFERENCES

[1] C. Cerny, *Hoppe-Seylers Z. Physiol. Chem.* **1911**, *73*, 371.
[2] H. Falk, *Angew. Chem. Int. Ed.* **1999**, *38*, 3116.
[3] R. C. Guedes, L. A. Eriksson, *J. Photochem. Photobiol. A: Chem.* **2005**, *172*, 293.
[4] J. Ulicny, A. Laaksonen, *Chem. Phys. Lett.* **2000**, *319*, 396.
[5] M. G. Siskos, M. I. Choudhary, A. G. Tzakos, *Tetrahedron* **2016**, *72*, 8287.
[6] P. Keša, M. Antalík, *Chem. Phys. Lett.* **2017**, *676*, 112.
[7] Z. Jendželovská, R. Jendželovský, B. Kuchárová, P. Fedoročko, *Front. Plant Sci.* **2016**, *7*, 560.
[8] S. Kasper, F. Caraci, B. Forti, F. Drago, E. Aguglia, *Eur. Neuropsychopharmacol.* **2010**, *20*, 747.
[9] U. Wölfle, G. Seelinger, C. Schempp, *Planta Med.* **2014**, *80*, 109.
[10] S. Yano, S. Hirohara, M. Obata, Y. Hagiya, S. Ogura, A. Ikeda, H. Kataoka, M. Tanaka, T. Joh, *J. Photochem. Photobiol.* **2011**, *12*, 46.
[11] L. Shen, H.-F. Ji, H.-Y. Zhang, *Bioorg. Med. Chem. Lett.* **2006**, *16*, 1414.
[12] B. C. De Simone, M. E. Alberto, N. Russo, M. Toscano, *J. Comput. Chem.* **2021**, *42*, 1803.
[13] J. Pirillo, G. Mazzone, N. Russo, L. Bertini, *J. Chem. Inf. Model.* **2017**, *57*, 234.
[14] G. Mazzone, B. C. De Simone, T. Marino, N. Russo, *J. Chem. Phys.* **2021**, *154*, 084113.
[15] J. A. Roque, P. C. Barrett, H. D. Cole, L. M. Lifshits, E. Bradner, G. Shi, D. von Dohlen, S. Kim, N. Russo, G. Deep, C. G. Cameron, M. E. Alberto, S. A. McFarland, *Inorg. Chem.* **2020**, *59*, 16341.
[16] M. E. Alberto, N. Russo, C. Adamo, *Chem.–Eur. J.* **2016**, *22*, 9162.
[17] E. Brémond, M. E. Alberto, N. Russo, I. Ciofini, C. Adamo, *Phys. Chem. Chem. Phys.* **2013**, *15*, 10019.
[18] M. E. Alberto, T. Marino, N. Russo, E. Sicilia, M. Toscano, *Phys. Chem. Chem. Phys.* **2012**, *14*, 14943.
[19] Y. Zhao, D. G. Truhlar, *Theor. Chem. Acc.* **2008**, *120*, 215.
[20] D. Andrae, U. Haussermann, M. Dolg, H. Stoll, H. Preuss, *Theor. Chim. Acta* **1990**, *77*, 123.
[21] A. V. Marenich, C. J. Cramer, D. G. Truhlar, *J. Phys. Chem. B* **2009**, *113*, 6378.
[22] M. J. Frisch, G. W. Trucks, H. B. Schlegel, G. E. Scuseria, M. Robb, J. R. Cheeseman, G. Scalmani, V. Barone, B. Mennucci, G. A. Petersson, *Gaussian 09*, *Revision D.01*, Gaussian, Wallingford, CT **2009**.
[23] DALTON. A Molecular Electronic Structure Program. Release Dalton 2011. http://daltonprogram.org/.
[24] S. Koseki, M. W. Schmidt, M. S. Gordon, *J. Phys. Chem. A* **1998**, *102*, 10430.
[25] K. Ruud, B. Schimmelpfennig, H. Ågren, *Chem. Phys. Lett.* **1999**, *310*, 215.
[26] A. D. Becke, *J. Chem. Phys.* **1993**, *98*, 5648.
[27] C. Lee, W. Yang, R. G. Parr, *Phys. Rev. B* **1988**, *37*, 785.
[28] C. Etzlstorfer, H. Falk, N. Muller, W. Schmitzberger, U. G. Wagner, *Monatsh Chem.* **1993**, *124*, 751.
[29] D. Freeman, F. Frolow, E. Kapinus, D. Lavie, D. Meruelo, Y. Mazur, *J. Chem. Soc. Chem. Commun.* **1994**, 891.
[30] J. G. Leonhartsberger, H. Falk, *Monatsh Chem.* **2002**, *133*, 167.
[31] S. M. Arabei, J. P. Galaup, P. Jardon, *Chem. Phys. Lett.* **1997**, *270*, 31.
[32] P. Jardon, N. Lazorchak, R. Gautron, *J. Chim. Phys.* **1986**, *83*, 311.
[33] A. P. Darmanyan, W. S. Jenks, D. Eloy, P. Jardon, *J. Phys. Chem. B* **1999**, *103*, 3323.
[34] D. Freeman, L. Konstantinovskii, Y. Mazur, *Photochem. Photobiol.* **2001**, *74*, 206.
[35] C. M. Marian, *Wiley Interdiscip. Rev. Comput. Mol. Sci.* **2012**, *2*, 187.
[36] S. Banfi, E. Caruso, S. Caprioli, L. Mazzagatti, G. Canti, R. Ravizza, M. Gariboldi, E. Monti, *Bioorg. Med. Chem.* **2004**, *12*, 4853.
[37] M. E. Alberto, T. Marino, A. D. Quartarolo, N. Russo, *Phys. Chem. Chem. Phys.* **2013**, *15*, 16167.
[38] M. A. El-Sayed, *Acc. Chem. Res.* **1968**, *1*, 8.

SUPPORTING INFORMATION

Additional supporting information can be found online in the Supporting Information section at the end of this article.

How to cite this article: B. C. De Simone, G. Mazzone, M. Toscano, N. Russo, *J. Comput. Chem.* **2022**, *43*(30), 2037. https://doi.org/10.1002/jcc.27002